# Provenance of intermediate waters in the western North Pacific deduced from thermodynamic imprint on $\delta^{13}C$ of DIC

Masashi Itou
Institute for Frontier Research on Earth Evolution, JAMSTEC, Yokosuka, Japan

Tsuneo Ono
Hokkaido National Fisheries Research Institute, Fisheries Research Agency, Kushiro, Japan

Shinichiro Noriki
Graduate School of Environmental Earth Science, Hokkaido University, Sapporo, Japan

Received 15 December 2002; revised 3 June 2003; accepted 11 July 2003; published 8 November 2003.

[1] Stable carbon isotopes of dissolved inorganic carbon ($\delta^{13}C_{DIC}$), together with phosphate concentrations ($PO_4^{3-}$) of the western North Pacific marginal area are presented. Although $\delta^{13}C_{DIC}$ controlled not only air-sea exchange but also biological activities, by subtracting $PO_4^{3-}$ as a biological factor from the $\delta^{13}C_{DIC}$, the thermodynamic imprint on the carbon isotopic composition ($\delta^{13}C_{as}$) is used as a conservative tracer. The linear relationship between $\delta^{13}C_{as}$ and temperature with the $\delta^{13}C_{as}$/temperature slope of $-0.104$‰/°C is observed in the North Pacific subtropical region. This relationship can be extended to the Weddell Sea deep waters. Therefore oceanic DIC is apparently in temperature-dependent isotopic equilibrium with atmospheric $CO_2$. To characterize each water mass, the "isotopically labeled temperature" ($T_{iso}$), which is derived from $\delta^{13}C_{as}$-temperature relationship obtained for the subtropical gyre water and Weddell Sea Water, is introduced. In contrast, the $\delta^{13}C_{as}$-temperature relationship is not necessarily linear for the northern Japan Sea Water, the Kuroshio-Oyashio Mixed Water and the Okhotsk Sea Water. This nonlinearity implies apparent air-sea carbon isotopic disequilibria resulting from water cooling without accompanying air-sea carbon isotope equilibrium. By using the potential temperature ($T_{pot}$) and the $T_{iso}$, the source waters constituting intermediate waters ($26.8\sigma_\theta$) have been estimated. The results clearly indicate that (1) the intermediate water in the southern Okhotsk Sea contains up to 20% Japan Sea Water, and that (2) "new" North Pacific Intermediate Water (NPIW) consists of Okhotsk Sea Water, subarctic gyre water, and "old" subtropical NPIW. *INDEX TERMS:* 4808 Oceanography: Biological and Chemical: Chemical tracers; 4283 Oceanography: General: Water masses; 4870 Oceanography: Biological and Chemical: Stable isotopes; *KEYWORDS:* carbon isotopes, isotope tracer, intermediate water, western North Pacific

**Citation:** Itou, M., T. Ono, and S. Noriki, Provenance of intermediate waters in the western North Pacific deduced from thermodynamic imprint on $\delta^{13}C$ of DIC, *J. Geophys. Res.*, *108*(C11), 3347, doi:10.1029/2002JC001746, 2003.

## 1. Introduction

[2] In the western North Pacific, the North Pacific Intermediate Water (NPIW) is defined as water with a salinity minimum and a density of $26.8\sigma_\theta$, [*Reid*, 1965; *Talley*, 1993]. The "new" NPIW appears in the "Kuroshio-Oyashio Mixed Water" region [*Talley*, 1997]; however, recently ventilated water contained in the NPIW is thought to originate in the Okhotsk Sea since densities $>26.8\sigma_\theta$ do not outcrop in the North Pacific (Figure 1).

[3] The source of the subsurface and intermediate waters in the Okhotsk Sea, which is one of the main constituents of the NPIW, has been a matter of considerable debate [*Wong et al.*, 1998; *Talley*, 1988; *Yasuda*, 1997]. *Wong et al.* [1998] suggested that a major constituent of this intermediate water could be derived by mixing shelf-derived water in the northern Okhotsk Sea and North Pacific Water. However, the Soya Warm Water (SWW) is also important for water-mass processes in the Okhotsk Sea since it provides salinity, which permits production of dense water [*Talley*, 1991]. By calculating mixing ratio with *T-S* and $O_2$-$\sigma_\theta$ diagram, *Watanabe and Wakatsuchi* [1998] suggested the Soya Warm Water, which is a branch of the Tsushima Warm Current in the Japan Sea (Figure 1), as one of the major source constituent. The SWW is relatively saline (>33.6 psu) [e.g., *Aota*, 1975], and the Forerunner of Soya Warm Water (FSWW) is modified SWW formed by convective mixing during a period of cooling off the western coast of Hokkaido (Figure 1) [*Fujii*

Copyright 2003 by the American Geophysical Union.
0148-0227/03/2002JC001746

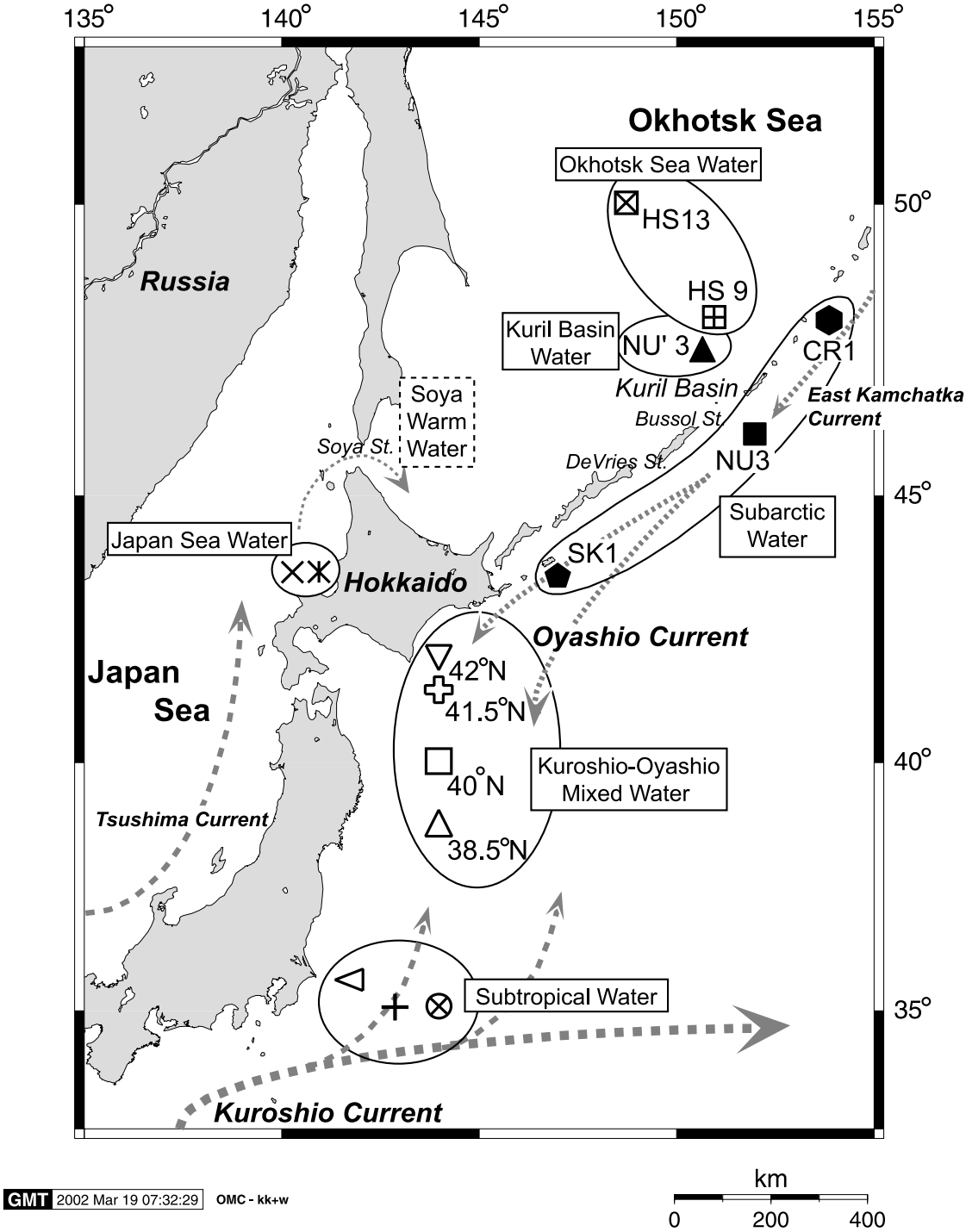


**Figure 1.** Location map of water sampling stations. Also shown are the water masses discussed in this paper. Arrows indicate major water currents. Stations HS9 and HS13 are sampling stations during the WOCE P01W cruise in September 1993 (http://whpo.ucsd.edu/data/onetime/pacific/p01/p01w/index.htm).

*and Sato*, 1979]. However, it is difficult to estimate the proportions and to the degree in which the SWW and FSWW contribute to the subsurface and intermediate depth waters in the Kuril Basin before exchange into the northwestern North Pacific. In the Okhotsk Sea, even though some chemical tracers have been employed to study water-mass processes around the Okhotsk Sea, e.g., $\Delta^{14}C$, CFCs, and $\delta^{18}O$ of water [*Tsunogai et al.*, 1995; *Wong et al.*, 1998; *Yamamoto et al.*, 2002], contributions of the Japan Sea Water to the Okhotsk Sea have not been evaluated with any chemical tracers.

[4] This paper outlines the use of a conservative chemical tracer to distinguish individual sources of intermediate waters around the western North Pacific in order to provide

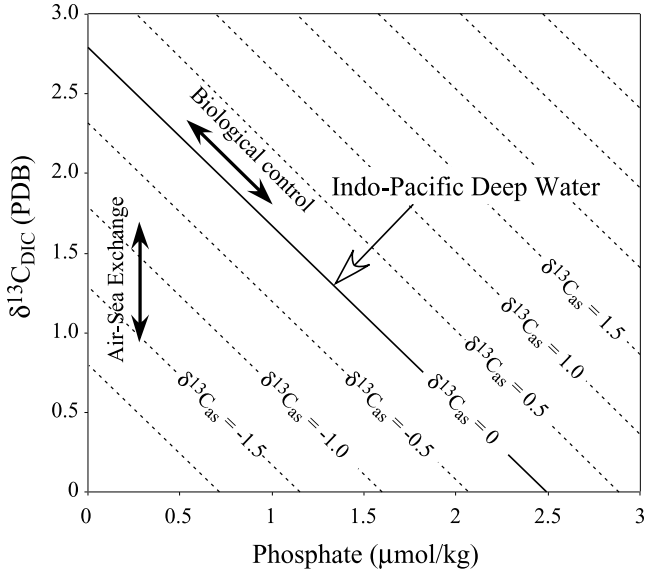


**Figure 2.** Schematic diagram of phosphate concentration versus $\delta^{13}C$ of DIC. Parallel lines represent "Redfield-driven biological fractionation," which reflects both the photosynthesis and the remineralization of organic matter. Air-Sea exchange fractionation is independent of biogenic activities, which is represented by phosphate concentration. By definition, water with $\delta^{13}C_{as}$ of 0‰ has the same air-sea exchange signature as mean ocean deep water. Positive (negative) $\delta^{13}C_{as}$ means an influence of air-sea exchange at cold (warm) temperatures.

further constraints on mixing processes associated with the formation of the NPIW.

## 2. Theoretical Background of $\delta^{13}C$

[5] The carbon isotopic ratios of oceanic, dissolved inorganic carbon ($\delta^{13}C_{DIC}$) is primarily controlled by biological activities such as photosynthesis and respiration [*Broecker and Peng*, 1982]. The $\delta^{13}C_{DIC}$ value rises or drops by 1.1‰ per 1 μM of $PO_4$, taken up or remineralized, respectively. If there is no air-sea fractionation of $\delta^{13}C_{DIC}$, then the following relationship between $\delta^{13}C_{DIC}$ and $PO_4$ is obtained [*Broecker and Maier-Reimer*, 1992]:

$$\delta^{13}C_{DIC} = -1.1PO_4 + 2.8. \quad (1)$$

[6] This relationship is observed in the deep Pacific and Indian waters, in which only biological processes affect the $\delta^{13}C_{DIC}$ concentrations. However, carbon isotope compositions of DIC in surface seawater can be affected by air-sea $CO_2$ exchange [*Broecker and Maier-Reimer*, 1992; *Charles and Fairbanks*, 1990]. By subtracting the biologically "predicted" $\delta^{13}C_{DIC}$, which is calculated by substituting the phosphate concentration in equation (1), from "measured" $\delta^{13}C_{DIC}$, the effect of air-sea $CO_2$ exchange, denoted as $\delta^{13}C_{as}$, is calculated as follows:

$$\delta^{13}C_{as} = \delta^{13}C_{DIC} - (-1.1PO_4 + 2.8). \quad (2)$$

[7] Schematic diagram of phosphate concentration versus $\delta^{13}C_{DIC}$ is illustrated in Figure 2. The magnitude of carbon isotope fractionation during air-sea gas exchange is a function of temperature [*Mook et al.*, 1974; *Zhang et al.*, 1995]. Accordingly, once a water mass is out of contact with the atmosphere, the thermodynamic imprint on oceanic $\delta^{13}C$ ($\delta^{13}C_{as}$) can be regarded as a conservative tracer (Figure 2). So far, the $\delta^{13}C_{as}$ has been a powerful tool in the paleoceanographic community [*Bickert and Wefer*, 1999; *Lynch-Stieglitz and Fairbanks*, 1994; *Lynch-Stieglitz et al.*, 1995]. Temperature-dependent isotopic equilibrium between oceanic $\delta^{13}C_{DIC}$ and atmospheric $\delta^{13}C_{CO_2}$ occurs on a timescale of more than 10 years [*Lynch-Stieglitz et al.*, 1995]. When surface waters are exposed to the atmosphere for a few decades, the $\delta^{13}C_{DIC}$ would approach apparent equilibrium with atmospheric $CO_2$. The specific temperature at which this air-sea $CO_2$ exchange occurred is hereafter denoted as $T_{iso}$, and a linear relationship between $\delta^{13}C_{as}$ and temperature is observed. Accordingly, we speculate that the $T_{iso}$ may empirically be deduced from the $\delta^{13}C_{as}$ if isotopic exchange between oceanic $\delta^{13}C_{DIC}$ and atmospheric $\delta^{13}C_{CO_2}$ occurred under relatively stable conditions, i.e., the effects of invasion and evasion were negligible for more than a decade. When the rapid penetration of surface water into the ocean interior occurs before temperature-dependent isotopic equilibrium is established, a linear relationship between temperature and $\delta^{13}C_{as}$ may no longer exist. Hence the relationship between temperature and $\delta^{13}C_{as}$ would provide crucial information on recent water-mass formation.

## 3. Materials and Methods

[8] Hydrographic observations were carried out with a conductivity-temperature-depth (CTD) sensor during cruises of the R/V *Soyo Maru* of National Research Institute of Fisheries Sciences in August 1997 and in April 1998, the R/V *Hokko Maru* of the Hokkaido National Fisheries Institute in the Fisheries Agency in August–September 1997 and the R/V *Oyashio Maru* of Hokkaido Central Fisheries in September 1997 and in April 1998. Sampling stations were located in the western North Pacific marginal area, including the Okhotsk Sea and the Japan Sea (Table 1 and Figure 1). The depth profiles of each station are listed in Table 1. All bottle data are reported in Appendix A.

[9] The nutrient samples were placed in polypropylene tubes and frozen on board ship until measurements could be conducted in the laboratory. Nutrient concentrations were analyzed with the aid of auto-analyzer (Bran Luebbe TRAACS 800). Special grade reagent of $Na_2HPO_4$ was used for primary standards of phosphate. Duplicate analysis was carried out for samples collected during the cruise of the *Soyo Maru* in August 1997. The difference of duplicate phosphate samples is 0.001–0.09 μmol/L. Relative standard deviation for duplicate samples is 1.6–1.9% for the range of phosphate concentration determined (Appendix A). Two data sets collected during WOCE cruise P01W are also presented in this paper. Precision and reproducibility for WOCE phosphate data are 0.4 and 1–2%, respectively. Stations HS9 and HS13 are the same as those presented in the work of *Wong et al.* [1998] and *Keigwin* [1998].

[10] The sampling and measurement of $\delta^{13}C_{DIC}$ were carried out following the procedure of *Itou et al.* [2001].

**Table 1.** Lists of Observations

| Water Mass | Station Name | Latitude | Longitude | Date |
|---|---|---|---|---|
| Subarctic Water | NU3 | 46°02′N | 152°02′E | September 1, 1997 |
| | CR1 | 48°10′N | 153°47′E | September 16, 1997 |
| | SK1 | 43°28′N | 147°02′E | August 23, 1997 |
| Okhotsk Sea Water | NU′3 | 47°30′N | 150°30′E | September 2, 1997 |
| | HS9 | 48°00′N | 150°42′E | September 6, 1997 |
| | HS13 | 49°59′N | 149°06′E | September 8, 1997 |
| Japan Sea Water | J33 August | 43°30′N | 140°40′E | September 26, 1997 |
| | J33 April | 43°30′N | 140°40′E | April 17, 1998 |
| Kuroshio-Oyashio Mixed Water | 38.5N August | 38°35′N | 143°58′E | August 24, 1997 |
| | 38.5°N April | 38°30′N | 144°00′E | April 26, 1997 |
| | 40°N August | 39°58′N | 144°04′E | August 24, 1997 |
| | 41°N April | 41°02′N | 143°59′E | April 25, 1998 |
| | 42°N August | 42°00′N | 144°01′E | August 22, 1997 |
| Subtropical Water | | 35°01′N | 143°59′E | August 26, 1997 |
| | | 35°51′N | 142°10′E | April 16, 1998 |
| | | 35°17′N | 143°12′E | April 18, 1998 |

All results are reported relative to PDB [*Craig*, 1957]. Replicate analytical precision of the full procedure, based on many replicates of standard surface seawater from Kuroshio, is better than 0.05‰ (±1σ). No duplicate sampling was conducted for $\delta^{13}C$. As the error included in $\delta^{13}C_{as}$ is derived from both phosphate and $\delta^{13}C_{DIC}$, errors included in $\delta^{13}C_{as}$ would be $\left(\sqrt{\sigma^2_{\delta^{13}C} + \left(\sigma_{PO_4^{3-}} 1.1\right)^2}\right.$ =)0.05 − 0.08‰(±1σ). Accordingly, differences larger than 0.10–0.16‰ (2σ) among samples are considered to be significant.

## 4. Results and Discussions

### 4.1. Water-Mass Distribution and Hydrography

[11] Figures 3 and 4 illustrate the variance in temperature and salinity in the various study areas, respectively. In the subtropical gyre water region (Figure 1), vertical *T*/*S* pro-

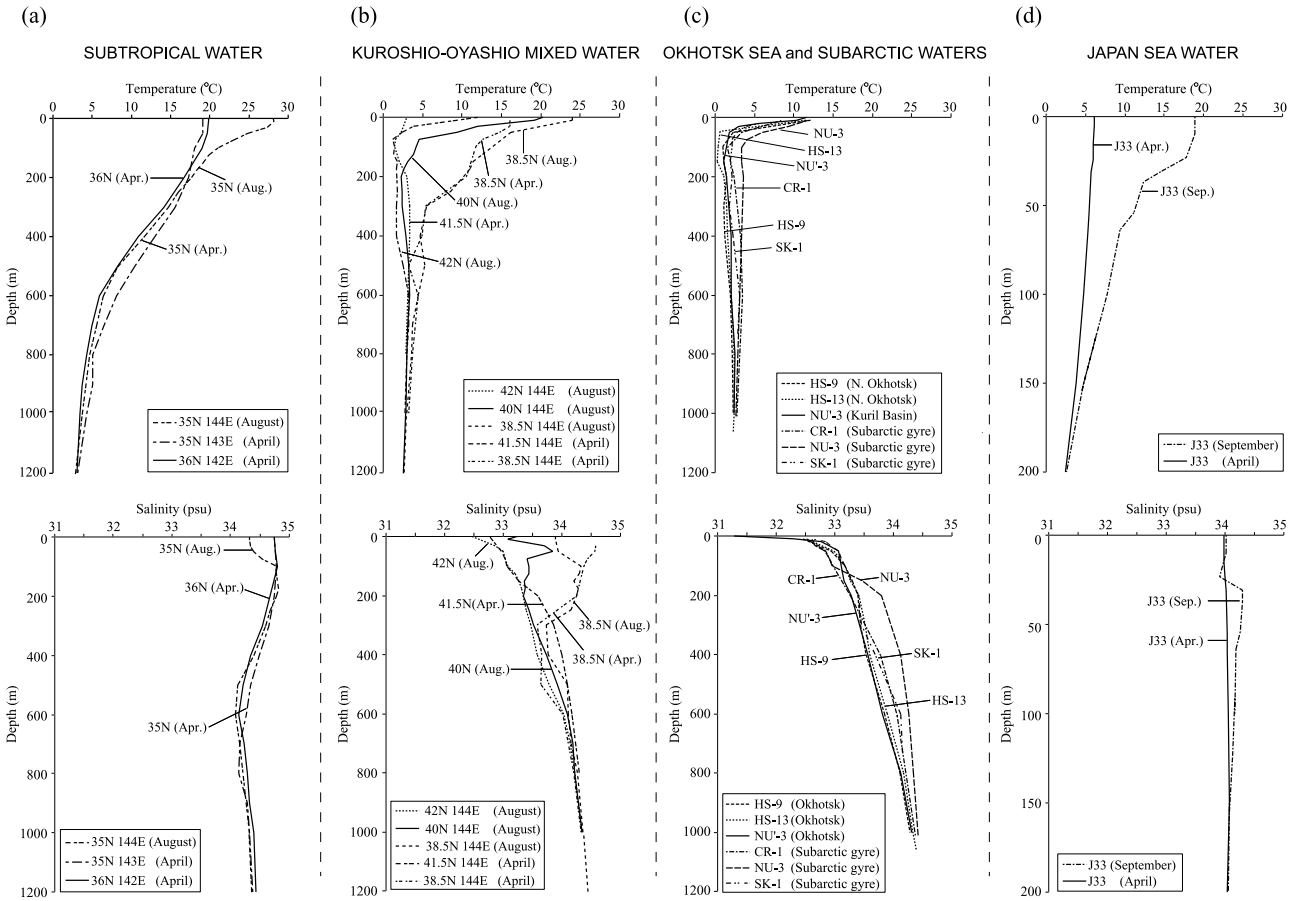


**Figure 3.** Vertical profiles of temperature and salinity on (a) subtropical gyre water, (b) Kuroshio-Oyashio Mixed Water, (c) Okhotsk Sea Water and subarctic gyre water, and (d) Japan Sea Water.

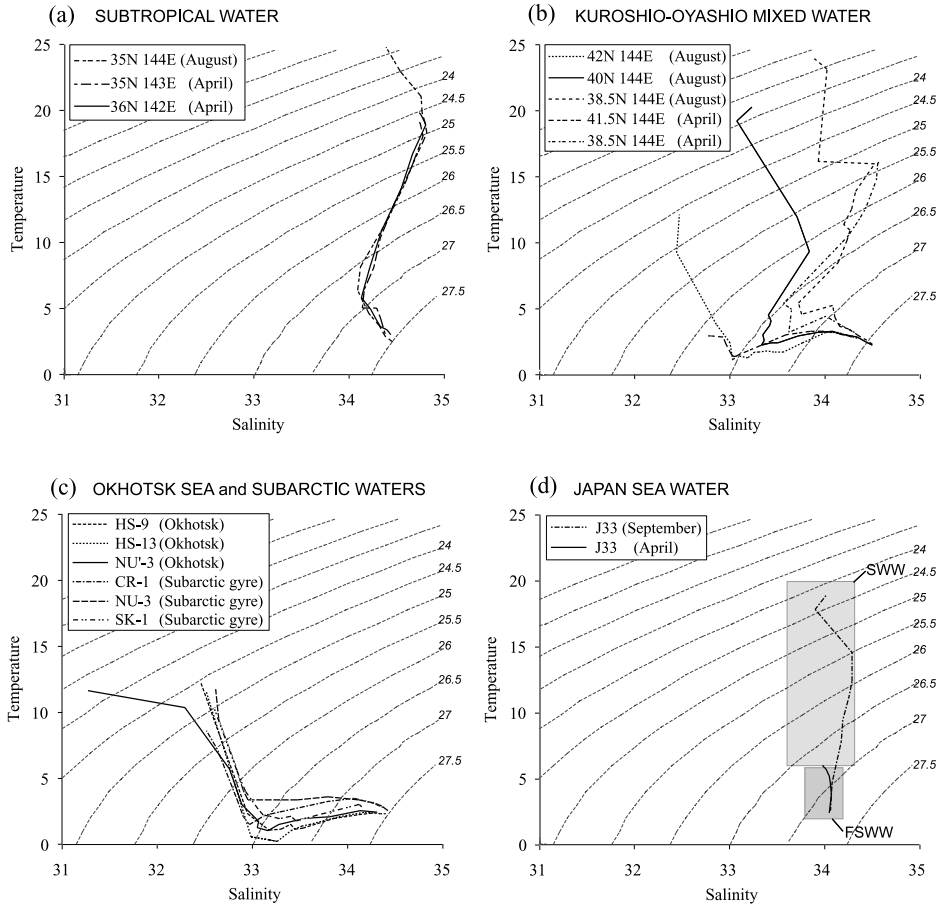


**Figure 4.** Temperature versus salinity diagrams on (a) subtropical gyre water, (b) Kuroshio-Oyashio Mixed Water, (c) Okhotsk Sea Water and subarctic gyre water, and (d) Japan Sea Water. Note that shaded area in Figure 4b indicates *T-S* ranges of the SWW and FSWW according to the classification by *Takizawa* [1982].

files show high surface water temperatures and little salinity fluctuation (Figure 3a). This *T*/*S* structure is typical of the subtropical gyre water. The smooth and obscure salinity minimum structures indicate that the ''old'' NPIW is distributed throughout this region [*Yasuda*, 1997; *Talley*, 1993] (Figures 3a and 4a).

[12] In the Kuroshio-Oyashio Mixed Water Region (Figure 1), temperature and salinity are intermediate between subtropical gyre water and subarctic gyre water (Figures 3a–3c and 4a–4c). Less-saline surface waters were identified at 41.5°N and 42°N, south of Hokkaido (Figure 3b). According to *Kawai* [1972], the monotonic increases in salinity and water temperature, at 5°C below 100 m water depth, at these two sites signify the dominance of Oyashio Water (Figure 3b). In contrast, the subsurface salinity minimum structure and relatively warm water at 100 m water depth documented at the southern sites (38.5°N and 40°N) (Figure 3b) are indicative of relatively new NPIW with a salinity lower than 34.0.

[13] In the Okhotsk Sea, salinity monotonically increases with depth (Figure 3c). Vertical water-temperature profiles were almost constant below 50 m, although the sea surface temperature (SST) was as high as 10°C due to increased insolation during summer. The temperature minima at subsurface water depths were as cold as 1°C at stations NU′3 and HS9 (Figures 3c and 4c). At station HS13, the minimum temperature was close to 0°C.

[14] Stations CR1, NU3, and SK1 (Figure 1) are also characterized by a monotonic increase in salinity with a fresh surface water, typical of subarctic gyre water in the western North Pacific (Figures 3c and 4c). The vertical temperature minimum was above 1.5°C at all three sites (Figures 3c and 4c). Accordingly, we consider that subarctic gyre water was dominant at these stations.

[15] The warm and saline water observed in the northern Japan Sea (station J33) reflects properties of the Tsushima Warm Current (Figures 1, 3d, and 4d) [e.g., *Chu et al.*, 2001]. One of the most pronounced water properties at this site is the formation of dense water, $26.7–26.9\sigma_\theta$, even at the surface in April (Figures 3d and 4d). Salinity change of 0.1 psu (34.0–34.1 psu) was observed in the upper 50 m of the water column from September to April. Temperature and salinity were 4°–5°C and 33.9–34.0, respectively, at 0–50 m water depths in the Soya Strait in April [*Takizawa*, 1982]. The *T*/*S* diagram for April and September show that the physical water properties at station J33 were very similar

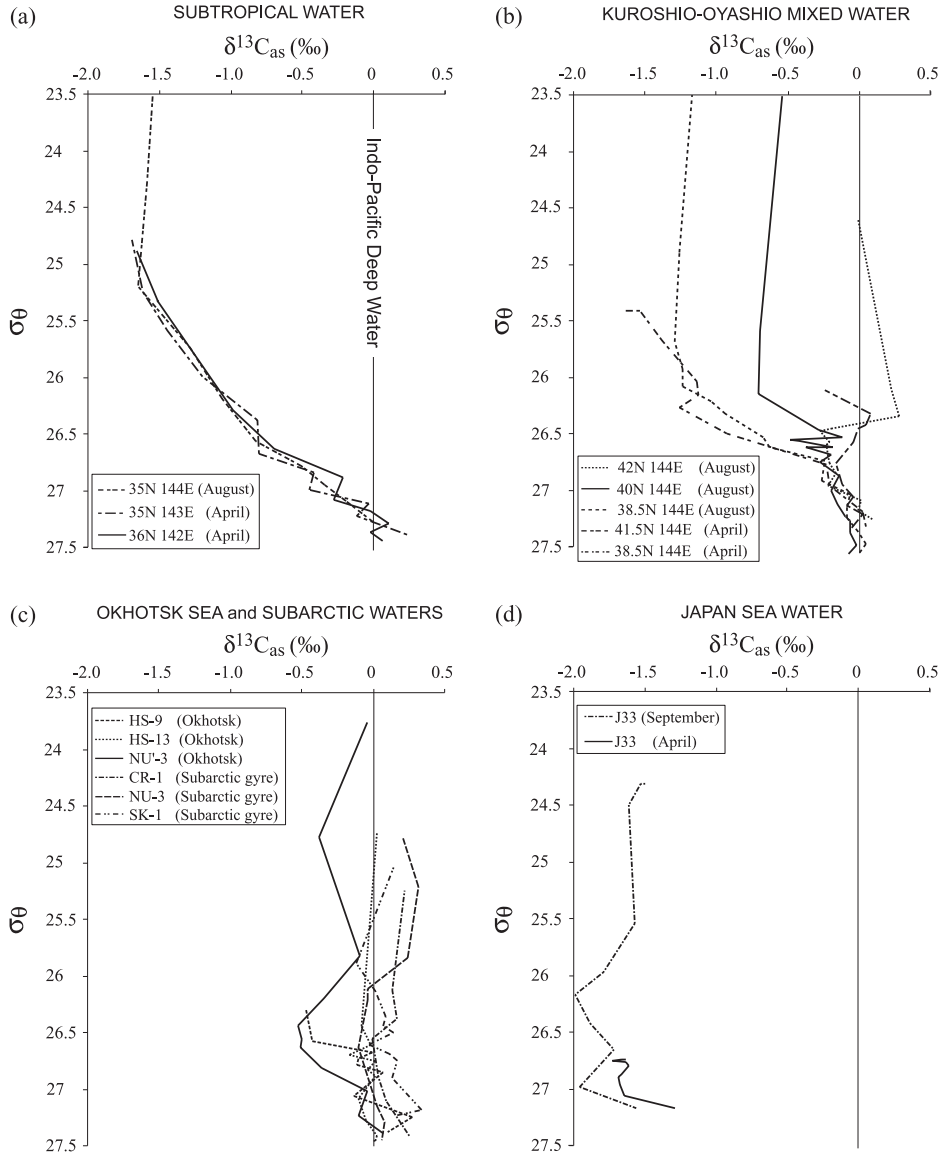


**Figure 5.** Vertical $\delta^{13}C_{as}$ profiles for (a) subtropical gyre water, (b) Kuroshio-Oyashio Mixed Water, (c) Okhotsk Sea Water and subarctic gyre water, and (d) Japan Sea Water.

to SWW and FSWW, respectively (Figure 4d) [*Takizawa*, 1982].

### 4.2. Temperature-$\delta^{13}C_{as}$ Relationship

[16] Figure 5 shows vertical profiles of $\delta^{13}C_{as}$ in the study area. The $\delta^{13}C_{as}$ is negatively deviated at the surface and increases monotonically with depth in the subtropical gyre water (Figure 5a). The $\delta^{13}C_{as}$ values of the Oyashio Water (41.5°N and 42°N) display small fluctuations throughout the water column (Figure 5b). Vertical profiles of $\delta^{13}C_{as}$ at 38.5°N are similar to those of the subtropical gyre waters (Figures 5a and 5b). At 42°N, negative $\delta^{13}C_{as}$ was observed only at a density range of 26.5–27.0$\sigma_\theta$ (Figure 5b). Similarly, a negative deviation of $\delta^{13}C_{as}$ structure was observed at 40°N (Figure 5b).

[17] At stations CR1, NU3, and SK1, characterized by subarctic gyre water, the mean $\delta^{13}C_{as}$ = 0 (Figure 5c). Deviations of $\delta^{13}C_{as}$, from zero, are small in the surface waters of both the Okhotsk Sea and subarctic gyre water (Figure 5c). In contrast to these small fluctuations of $\delta^{13}C_{as}$ in the surface water (<50 m), $\delta^{13}C_{as}$ of intermediate water depths (50–400 m) in the Kuril Basin (station NU′3) displays a minimum at 26.2–26.8$\sigma_\theta$ (Figure 5c). Similar negative $\delta^{13}C_{as}$ shifts are observed in the intermediate waters (50–100 m) of the Okhotsk Sea at station HS9 (26.3–26.5$\sigma_\theta$,). Such negative $\delta^{13}C_{as}$ shifts at subsurface and intermediate waters in the high-latitude oceanic area are difficult to explain. Neither large biological isotopic fractionation at high latitude [*Rau et al.*, 1989] nor thermodynamic isotopic fractionation during cold winters could shift the $\delta^{13}C_{as}$ toward such negative values. Although a portion of the East Kamchatka Current, characterized by subarctic gyre water, enters the Okhotsk Sea [e.g., *Stabeno et al.*, 1994], negative $\delta^{13}C_{as}$ anomalies in the Okhotsk Sea cannot be fully explained by the $\delta^{13}C_{as}$ ratio of this water body. Hence an alternative explanation must be given.

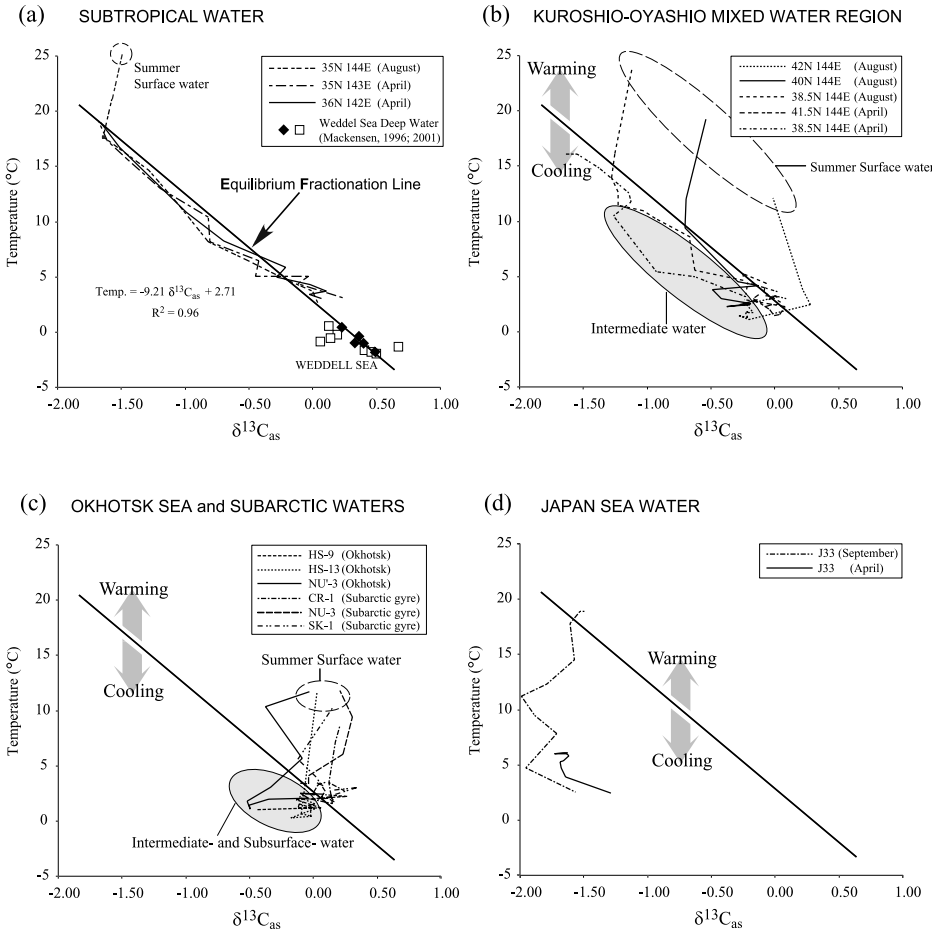


**Figure 6.** The $\delta^{13}C_{as}$ versus temperature diagrams for (a) subtropical gyre water and Weddell Sea Water ([*Mackensen et al.*, 1996] (solid diamond) and 2001 (open square)), (b) Kuroshio-Oyashio Mixed Water Region, (c) Okhotsk Sea Water and subarctic gyre water, and (d) Japan Sea Water. Note that mean values are used for Weddell Sea Water.

[18] In the Japan Sea (station J33) the $\delta^{13}C_{as}$ profile was vertically uniform throughout the water column but displays negative deviations (Figure 5d). This suggests that the long-term air-sea isotopic exchange history of the water at J33 is similar to that of surface water in the North Pacific subtropical gyre (Figures 5a and 5d). In spite of substantial temperature change from September 1997 to April 1998, only a slight shift in $\delta^{13}C_{as}$ of the surface water was observed at station J33 (Figure 5d). This evidence confirms that $\delta^{13}C_{as}$ preserves long-term thermodynamic imprints. In addition, if waters at station J33 were assumed to be the precursor of the SWW and FSWW, the negative $\delta^{13}C_{as}$ anomalies found at stations HS9 and NU′3 in the Okhotsk Sea could be attributed to the penetration of the SWW and/or FSWW (Figures 5c and 5d).

[19] In Figure 6, the $\delta^{13}C_{as}$ is plotted against water temperature. *Mook et al.* [1974] and *Zhang et al.* [1995] experimentally determined the equilibrium $^{13}C$ fractionation between DIC and $CO_2$ in air ($\varepsilon_{DIC\text{-}gas}$). Their empirically obtained results show a linear temperature-dependent $\varepsilon_{DIC\text{-}gas}$ of $-0.105$‰/°C. In the subtropical gyre water, the $\delta^{13}C_{as}$ appears linearly related to temperature throughout the water column, except for surface waters in which seasonal temperature change is prominent (Figure 6a). Seasonal SST was lowered by 8°C from August 1997 to April 1998 in the subtropical gyre water (Figure 3a). If temperature-dependent air-sea isotopic equilibrium was assumed, this cooling would correspond to an isotopic shift of +0.84‰. However, the $\delta^{13}C_{as}$ shift was no greater than 0.2‰ (Figure 5a and Appendix A). This suggests that the $\delta^{13}C_{as}$ is not sensitive to short-term SST fluctuations. Therefore the $\delta^{13}C_{as}$ of surface waters should record an estimation of the temporally averaged temperature to which surface waters were exposed. In the subtropical gyre, as surface-water-cooling promotes vertical mixing of the upper water column during winter, water densities lower than $26.8\sigma_\theta$ can outcrop in the western North Pacific [*Reid*, 1969; *Levitus*, 1982]. This means that DIC in the subtropical western North Pacific waters, whose densities are less than $26.8\sigma_\theta$, have a chance to approach isotopic equilibrium with atmospheric $CO_2$.

[20] As can be seen in Figure 6a, the linear $\delta^{13}C_{as}$-temperature relationship is also applicable to the deep waters. Since the Pacific Deep Water originates from the Antarctic Ocean, this linearity may be extended to the Southern Ocean using the Weddell Sea as an example (Figure 6a) [*Mackensen et al.*, 1996; *Mackensen*, 2001]. This continuity may indicate that the degree of equilibrium of $\delta^{13}C_{as}$ at the subtropical North Pacific is relatively

uniform from surface to subsurface and is comparable to that at the Weddell Sea surface water. The $\delta^{13}C_{as}/T$ slope obtained for the subtropical gyre water and the Weddell Sea Water is as follows:

$$\delta^{13}C_{as}(‰) = -0.104T(°C) + 0.269 \quad (3)$$

$$r^2 = 0.96,\ n = 44.$$

[21] The $\delta^{13}C_{as}/T$ slope of $-0.104$‰/°C obtained is consistent with experimentally determined temperature-dependent $^{13}C$ fractionation between DIC in seawater and $CO_2$ within the atmosphere [*Mook et al.*, 1974; *Zhang et al.*, 1995]. In addition, the $\delta^{13}C_{as}$ in the surface water increases with decreasing SST in the mid-latitude Pacific [*Lynch-Stieglitz et al.*, 1995, Figures 5b and 5d therein]. Although kinetic fractionation during air-sea $CO_2$ exchange is not rigorously discussed here, the temperature-dependent equilibration would mask the effects of kinetic fractionation [*Lynch-Stieglitz et al.*, 1995]. Since surface waters are replaced on faster timescales, there is no region where surface ocean DIC is in complete isotopic equilibrium with the atmosphere. Even so, it is most likely that the $\delta^{13}C_{as}$ can have linear relationship to temperature if surface waters circulate for a relatively long time giving the oceanic carbon ample time, i.e., decadal or longer timescales, to equilibrate isotopically with atmosphere. Accordingly, we regard equation (3) as an apparent "Equilibrium Fractionation Line (E-F Line)" commonly observed in the Antarctic Deep Water and the subtropical western North Pacific. Since the Pacific Deep Water upwells at high latitude, surface waters in the mid- and high-latitude Pacific may originally follow this E-F Line. Therefore we assume that the $\delta^{13}C_{as}$-temperature relationship of all water masses examined here were originally in accordance with the E-F Line.

[22] The $\delta^{13}C_{as}$-temperature relationship of subtropical gyre water does not form a perfectly straight line (Figure 6a). Significant anomalies are observed at a temperature range of 5°–9°C, which corresponds to a water density of 26.6–27.0$\sigma_\theta$, similar to that of the NPIW (Figure 6a). Although we do not have convincing explanation for anomalies below 5°C, which corresponds to a water density >27.0$\sigma_\theta$, the modified Antarctic Intermediate Water (AAIW) might account for this anomaly (Figure 6a). Similarly, the nonlinear $\delta^{13}C_{as}$-temperature relationship is also observed in the Mixed Water Region (Figure 6b), and the subsurface and intermediate waters of the Okhotsk Sea (stations NU′3 and HS9) (Figure 6c) also display significant deviations. These deviations infer that water-cooling took place so quickly during winter that the $\delta^{13}C_{as}$ could not reach air-sea thermodynamic equilibrium (Figures 6b and 6c). Therefore we speculate that surface-water-cooling of short duration, several months at longest, without accompanying carbon isotope equilibrium occurred during formation of the NPIW. The $\delta^{13}C_{as}$-temperature relationship in the Japan Sea is largely deviated from the E-F line, except summer surface water (Figure 6d). Since the sampling site is located on the downstream of the Tsushima Warm Current, surface water should have approached air-sea isotopic equilibrium at relatively high temperature during summer. In fact, in contrast to relatively large temperature range of 3°–19°C resulting from intense cooling of the Tsushima Warm Current water under the East Asian Winter Monsoon regime, the $\delta^{13}C_{as}$ in the Japan Sea only varies from $-2.0$ to $-1.2$‰ (Figures 3d, 5d, and 6d).

[23] Since the $\delta^{13}C_{as}$ is dependent on the mean temperature during which waters were in contact with the atmosphere, an isotopically labeled temperature can be calculated if temperature-independent isotope fractionation were negligible.

$$T_{iso}(°C) = 9.21\delta^{13}C_{as}(‰) + 2.71. \quad (3')$$

[24] Here $T_{iso}$ is the isotopically labeled temperature. It is assumed that any disagreement of in situ potential temperature with this apparent temperature is derived from the temperature-dependent isotopic disequilibria. Although both temperature and $\delta^{13}C_{as}$ are treated as conservative, this assumption is valid only for waters out of touch with the atmosphere. Because the error included in $\delta^{13}C_{as}$ is 0.05–0.08‰, that for $T_{iso}$ ($\pm1\sigma$), which is calculated with $\delta^{13}C_{as}$, will be 0.46°–0.74°C ($= 9.21\sqrt{\sigma^2_{\delta^{13}C} + \left(\sigma_{PO_4^{3-}} 1.1\right)^2}$).

### 4.3. Discrepancy of the Potential Temperature From the Isotopically Labeled Temperature

[25] Here we focus on disagreement between potential temperature ($T_{pot}$) and isotopically labeled temperature ($T_{iso}$). Figure 7 displays vertical profiles of the $\Delta T$ ($= T_{pot} - T_{iso}$). When the DIC is in temperature-dependent isotopic equilibrium with atmospheric $CO_2$, the $T_{iso}$ should be equal to the $T_{pot}$, i.e., $\Delta T = 0$. Significantly large $\Delta T$ represent changes in potential temperature without accompanying carbon isotopic equilibrium.

[26] The $\Delta T$ is not largely deviated from zero, except surface water, in the subtropical gyre water (Figure 7a). In contrast, distinct negative $\Delta T$ are discerned mainly at density ranges from 26.1 to 27.0$\sigma_\theta$ in the Mixed Water Region (Figure 7b). Interestingly, negative $\Delta T$ are also observed in the Okhotsk Sea at a density range of 26.2–27.3$\sigma_\theta$ (Figure 7c). The degree of negative shift is greater in the southern Okhotsk sites (stations HS9 and NU′3) than the northern site (station HS13) (Figure 7c). Since the $\delta^{13}C_{as}$ at NU′3 and HS9 are more negatively deviated, the mixing of SWW/FSWW, accompanied by rapid water-cooling, probably occurred within several months, could account for these deviations (Figures 5c, 5d, 7c, and 7d). On the other hand, negative $\Delta T$ are observed at intermediate water depths (Figure 7c), though the $\delta^{13}C_{as}$ at station HS13 is similar to that of the North Pacific subarctic gyre waters rather than that of the Japan Sea Water (Figure 5c). Intense water-cooling during winter, which would occur in several months timescale, could have promoted the formation of cold subsurface waters without changing the $\delta^{13}C_{as}$ at station HS13. Therefore the intrusion of the Japan Sea Water and intense cooling of surface water, followed by subduction into subsurface water depths, account for the negative $\Delta T$ in the southern Okhotsk Sea.

[27] In the subarctic region, the positive shifts of $\Delta T$ at the sea surface are most likely due to the samples having been collected in summer (Figure 7c). The $\Delta T$ below the 26.2$\sigma_\theta$ isopycnal surface was not considerably

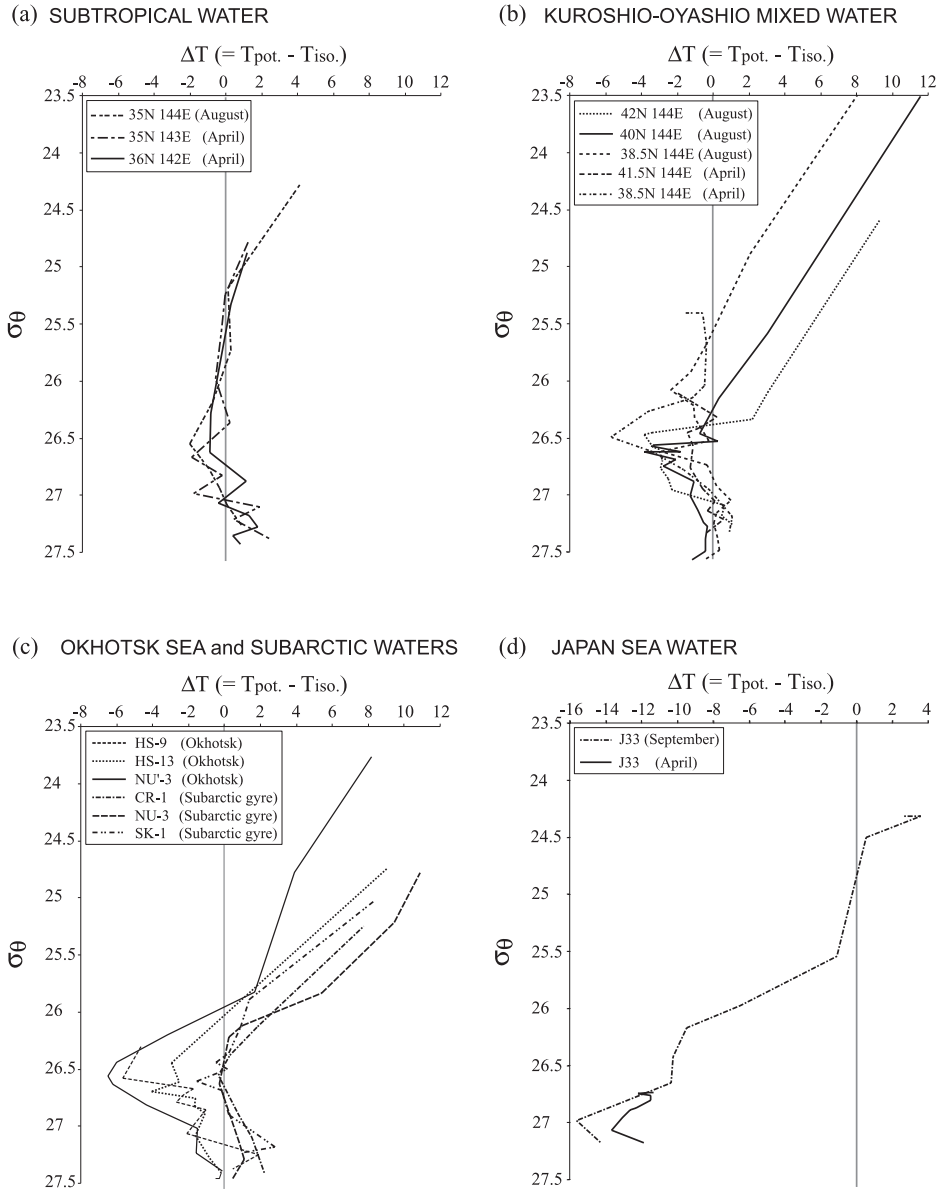


**Figure 7.** Vertical $\Delta T$ profiles for (a) subtropical gyre water, (b) Kuroshio-Oyashio Mixed Water, (c) Okhotsk Sea Water and subarctic gyre water, and (d) Japan Sea Water.

different from zero, implying the predominance of old deep waters having been out of touch with the atmosphere (Figure 7c).

[28] In the Japan Sea, the $\Delta T$ indicates cooling of $-11°$ to $-13°$C throughout the water column (0–200 m) in April (Figure 7d). The cooling effect is limited below the $25.5\sigma_\theta$ isopycnal surface in September. Such distinct negative $\Delta T$ values in the Japan Sea can adequately explain those anomalies observed in the southern Okhotsk Sea (stations NU′3 and HS9) if mixing of the Japan Sea Water to the subsurface water depths in the southern Okhotsk Sea had occurred (Figures 7c and 7d).

### 4.4. Provenance of Intermediate Waters

[29] In this section, we discuss the origin of intermediate waters along the $26.8\sigma_\theta$ isopycnal surface with respect to $T_{pot}$ and $T_{iso}$. Since waters on the exact $26.8\sigma_\theta$ were not always sampled, $T_{pot}$ and $T_{iso}$ at this isopycnal surface were estimated by interpolation.

[30] Figure 8 illustrates the $T_{pot}$-$T_{iso}$ relationship for the $26.8\sigma_\theta$ isopycnal surface. In subtropical gyre water and subarctic gyre water, the $T_{iso}$ is similar to the $T_{pot}$, i.e., the data points plot along the E-F Line, indicating that the $26.8\sigma_\theta$ isopycnal surface has not recently outcropped in the subarctic gyre of the North Pacific.

[31] The most prominent discrepancy between the $T_{pot}$ ($5.8°-6.4°$C) and the $T_{iso}$ ($17.3°-19.2°$C) is observed in the Japan Sea (station J33) (Figure 8). This discrepancy most likely results from the rapid cooling of surface water during the winter monsoon regime. Similarly, small but significant differences between the $T_{pot}$ and the $T_{iso}$ are observed in the Okhotsk Sea (stations NU′3, HS9, and HS13) (Figure 8). The $T_{pot}$-$T_{iso}$ for the Kuril Basin (station NU′3) plots on a mixing line between the Japan Sea Water

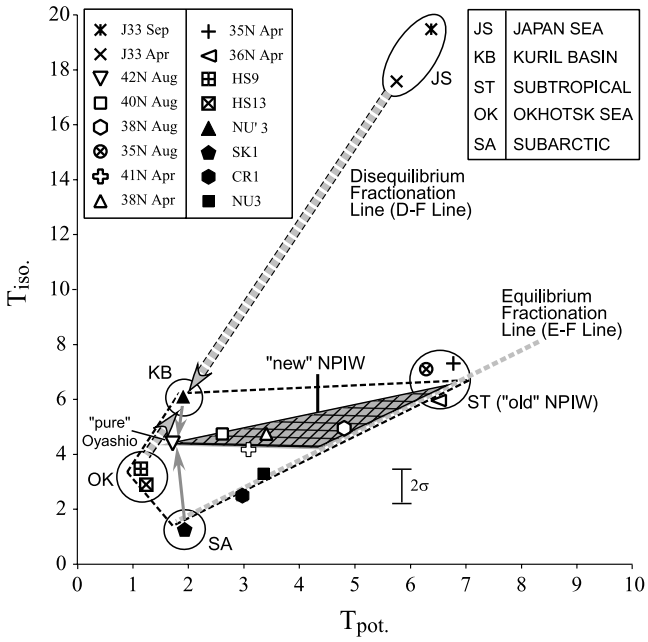


**Figure 8.** $T_{pot}$-$T_{iso}$ relationship on the 26.8$\sigma_\theta$ isopycnal surface. JS, Japan Sea Water; OK, Okhotsk Sea Water; ST, subtropical gyre Water; SA, subarctic gyre water; KB, Kuril Basin Water.

(station J33) and the northern Okhotsk Sea Water (station HS13) (Figure 8). The line connecting stations J33 and HS13 has slope of $T_{iso}/T_{pot}$ = 3:1 (Figure 8). This slope implies that one third of DIC reached apparent equilibrium with atmospheric $CO_2$ at an in situ potential temperature. We define this slope as an apparent "Disequilibrium Fractionation Line (D-F Line)", although not all these disequilibria are likely to be due to temperature-dependent isotopic fractionation. Since the $\delta^{13}C_{as}$ values on the 26.8$\sigma_\theta$ isopycnal surface at station HS13 are not largely different from that in the subarctic gyre water (Figure 5c), intense water-cooling in the northern Okhotsk Sea may have uncoupled the $T_{pot}$ from $T_{iso}$. The $T_{pot}$-$T_{iso}$ for the Kuril Basin (station NU′3) plots between the Japan Sea Water and the northern Okhotsk Sea Water (station HS13) (Figure 8). This implies that the subsurface water on the 26.8$\sigma_\theta$ isopycnal surface in the Kuril Basin (station NU′3) is formed by the mixing of the SWW/FSWW (station J33) and northern Okhotsk Sea Water (HS13). By calibrating a box model with potential temperature, salinity, and CFC data, *Wong et al.* [1998] estimated that intermediate water (26.8$\sigma_\theta$) at station HS13 consists of northern Shelf-derived Water (40%) and the North Pacific water (60%). However, they explained the formation of the intermediate water only with two water sources and inferred the necessity of contribution of Japan Sea Water through the Soya Strait. Here assuming that the intermediate water at station NU′3 was formed by a mixture of Okhotsk Sea Intermediate Water (HS13) and SWW/FSWW (station J33), the Japan Sea Water must account for 18–20% (Figure 8). Our result is coincident with the estimation reported by *Watanabe and Wakatsuchi* [1998], in which they calculated a mixing ratio of 1:4 between FSWW and northwestern Okhotsk water by using *T-S* and $O_2$-$\sigma_\theta$ diagram.

[32] The $T_{pot}$-$T_{iso}$ at 42°N (August) is located between the stations NU′3 and HS13 on the D-F line (Figure 8). The *T*/*S* property signifies that this site must represent "pure Oyashio Water" (Figures 3b and 4b). This water body consists of Okhotsk Sea Water and subarctic gyre water [e.g., *Yasuda*, 1997]. If waters at stations SK1 and NU′3 were assumed as end-members for subarctic gyre water and Okhotsk Sea Water, respectively, a mixing ratio of NU′3:SK1 = 2:1 is obtained for pure Oyashio Water (Figure 8). This mixing ratio is consistent with that reported for 26.8$\sigma_\theta$ by *Yasuda* [1997], in which he estimated the ratio from the averaged potential temperature profile *Yasuda* [1997, Table 2].

[33] It is interesting to note that all the $T_{pot}$-$T_{iso}$ values on the 26.8$\sigma_\theta$ isopycnal surface of the Mixed Water Region are located within the tetragon enclosed by subtropical gyre water (ST), subarctic gyre water (SA), Okhotsk Sea Water (OK), and Kuril Basin Water (KB) (Figure 8). Assuming isopycnal mixing on the 26.8$\sigma_\theta$ [e.g., *Ono et al.*, 1998], the new NPIW can be expressed by Kuril Basin Water (KB), subarctic gyre water (SA), and subtropical gyre water (ST) (Figure 8). Apparent relative contribution of each end-member to the new NPIW is estimated (Table 2). The Kuril Basin Water (KB) is the main source of the new NPIW except 38.5°N (August) (Table 2). Also, the contribution of Kuril Basin (KB) water to the new NPIW is estimated to be larger than subarctic gyre water (SA) (Table 2). For 38.5°N (August), the $T_{pot}$-$T_{iso}$ plot indicates that waters originating from the Okhotsk Sea did not reach this site. This infers that during summer 1997, the new NPIW was formed by isopycnal mixing of subarctic gyre water and subtropical gyre water (old NPIW) at 38.5°N (Figure 8).

## 5. Conclusions

[34] In this study, we examined the utility of the $\delta^{13}C_{as}$ as a conservative tracer in the western North Pacific marginal area. With the aid of $\delta^{13}C_{as}$, we have confirmed the southern Okhotsk Sea Water (NU′3) on the 26.8$\sigma_\theta$ isopycnal surface contains up to 20% Japan Sea Water (J33), renamed as the SWW or the FSWW, is one of the main constituents of subsurface waters in the southern Okhotsk Sea. This result sustains the earlier findings of *Watanabe and Wakatsuchi* [1998].

[35] $T_{pot}$-$T_{iso}$ analysis indicates that the new NPIW is composed of a mixture among Okhotsk Sea Water, subarctic gyre water, and subtropical gyre water (old NPIW). However, since the new NPIW at 38.5°N did not contain water from the Okhotsk Sea Water in summer 1997, contributions of fresh water from the Okhotsk Sea to the subtropical North Pacific must have been negligible during this period.

**Table 2.** Relative Contribution of the Kuril Basin Water, Subarctic Gyre Water, and Subtropical Gyre Water to the New NPIW at 26.8$\sigma_\theta$ Isopycnal Surface

| Sampling Location | Month | Kuril Basin Water, % | Subarctic Water, % | Subtropical Water ("Old" NPIW), % |
|---|---|---|---|---|
| 38.5°N | August | 0 | 35 | 65 |
| 40°N | August | 55 | 25 | 20 |
| 42°N | August | 67 | 33 | 0 |
| 38.5°N | April | 49 | 25 | 26 |
| 41°N | April | 45 | 32 | 23 |

**Table A1.** Station Data

| Station | Pot. Density $\sigma_\theta$ | Depth, m | $T_{pot}$, °C | Salinity, psu | $\delta^{13}C$, ‰ PDB | $PO_4^{3-}$, μmol/kg | Error ±1σ | $\delta^{13}C_{as}$, ‰ | Error ±1σ | $T_{iso}$, °C | ΔT, °C | Error ±1σ |
|---|---|---|---|---|---|---|---|---|---|---|---|---|
| SK1 | 25.02 | 10 | 10.34 | 32.60 | 1.92 | 0.94 | – | 0.15 | 0.05 | 1.9 | 8.43 | 0.49 |
| | 25.89 | 20 | 5.65 | 32.84 | 1.43 | 1.14 | – | −0.12 | 0.05 | 4.3 | 1.37 | 0.51 |
| | 26.14 | 30 | 3.99 | 32.93 | 1.11 | 1.55 | – | 0.02 | 0.06 | 3.1 | 0.91 | 0.54 |
| | 26.36 | 50 | 2.72 | 33.06 | 0.82 | 1.88 | – | 0.09 | 0.06 | 2.5 | 0.25 | 0.58 |
| | 26.44 | 75 | 2.19 | 33.11 | 0.68 | 1.99 | – | 0.07 | 0.06 | 2.7 | −0.47 | 0.59 |
| | 26.50 | 100 | 2.16 | 33.18 | 0.54 | 2.18 | – | 0.14 | 0.07 | 2.0 | 0.16 | 0.62 |
| | 26.60 | 150 | 1.93 | 33.29 | 0.32 | 2.23 | – | −0.03 | 0.07 | 3.5 | −1.55 | 0.62 |
| | 26.69 | 200 | 2.12 | 33.41 | 0.19 | 2.48 | – | 0.11 | 0.07 | 2.2 | −0.13 | 0.66 |
| | 26.75 | 300 | 1.78 | 33.45 | 0.06 | 2.64 | – | 0.16 | 0.07 | 1.8 | −0.02 | 0.68 |
| | 26.89 | 400 | 2.29 | 33.68 | −0.15 | 2.80 | – | 0.13 | 0.08 | 2.1 | 0.23 | 0.70 |
| | 27.18 | 600 | 3.08 | 34.12 | −0.52 | 3.33 | – | 0.34 | 0.08 | 0.3 | 2.80 | 0.78 |
| | 27.22 | 730 | 2.89 | 34.16 | −0.63 | 3.27 | – | 0.17 | 0.08 | 1.8 | 1.12 | 0.77 |
| NU′3 | 23.76 | 0 | 11.68 | 31.28 | 2.37 | 0.36 | – | −0.03 | 0.05 | 3.5 | 8.17 | 0.46 |
| | 24.78 | 10 | 10.38 | 32.30 | 1.68 | 0.68 | – | −0.37 | 0.05 | 6.5 | 3.89 | 0.48 |
| | 25.83 | 30 | 5.66 | 32.76 | 1.09 | 1.48 | – | −0.09 | 0.06 | 4.0 | 1.69 | 0.54 |
| | 26.20 | 50 | 3.02 | 32.89 | 0.79 | 1.52 | – | −0.34 | 0.06 | 6.2 | −3.17 | 0.54 |
| | 26.43 | 76 | 1.77 | 33.06 | 0.66 | 1.48 | – | −0.52 | 0.06 | 7.7 | −5.96 | 0.54 |
| | 26.57 | 151 | 1.06 | 33.16 | 0.38 | 1.75 | – | −0.50 | 0.06 | 7.5 | −6.49 | 0.56 |
| | 26.63 | 202 | 1.45 | 33.28 | 0.23 | 1.88 | – | −0.51 | 0.06 | 7.6 | −6.19 | 0.58 |
| | 26.82 | 403 | 1.98 | 33.56 | −0.13 | 2.34 | – | −0.35 | 0.07 | 6.3 | −4.33 | 0.64 |
| | 27.01 | 605 | 2.05 | 33.81 | −0.40 | 2.87 | – | −0.04 | 0.08 | 3.6 | −1.52 | 0.71 |
| | 27.24 | 807 | 2.52 | 34.13 | −0.48 | 2.89 | – | −0.10 | 0.08 | 4.1 | −1.58 | 0.71 |
| | 27.39 | 1010 | 2.42 | 34.31 | −0.44 | 3.02 | – | 0.08 | 0.08 | 2.5 | −0.12 | 0.73 |
| NU3 | 24.78 | 10 | 11.76 | 32.62 | 1.93 | 0.98 | – | 0.21 | 0.05 | 1.4 | 10.37 | 0.49 |
| | 25.22 | 30 | 9.40 | 32.65 | 1.84 | 1.16 | – | 0.31 | 0.06 | 0.5 | 8.88 | 0.51 |
| | 25.84 | 50 | 5.98 | 32.83 | 1.43 | 1.46 | – | 0.24 | 0.06 | 1.1 | 4.85 | 0.53 |
| | 26.12 | 76 | 4.04 | 32.91 | 0.81 | 1.78 | – | −0.03 | 0.06 | 3.5 | 0.50 | 0.57 |
| | 26.22 | 101 | 3.33 | 32.95 | 0.62 | 1.95 | – | −0.04 | 0.06 | 3.5 | −0.22 | 0.59 |
| | 26.63 | 151 | 3.35 | 33.46 | 0.03 | 2.43 | – | −0.10 | 0.07 | 4.1 | −0.75 | 0.65 |
| | 26.87 | 202 | 3.56 | 33.80 | | 2.95 | – | | | | | |
| | 27.15 | 403 | 3.42 | 34.12 | −0.67 | 3.17 | – | 0.02 | 0.08 | 3.0 | 0.38 | 0.76 |
| | 27.29 | 605 | 3.12 | 34.27 | −0.53 | 3.10 | – | 0.08 | 0.08 | 2.5 | 0.59 | 0.75 |
| | 27.38 | 807 | 2.88 | 34.35 | | 3.17 | – | | | | | |
| | 27.46 | 1010 | 2.60 | 34.42 | −0.53 | 3.09 | – | 0.07 | 0.08 | 2.7 | −0.05 | 0.74 |
| CR1 | 25.25 | 10 | 8.55 | 32.52 | 1.93 | 0.99 | – | 0.22 | 0.05 | 1.3 | 7.21 | 0.49 |
| | 26.13 | 50 | 3.41 | 32.84 | 0.97 | 1.78 | – | 0.13 | 0.06 | 2.1 | 1.32 | 0.57 |
| | 26.38 | 101 | 1.56 | 32.97 | 0.69 | 2.07 | – | 0.16 | 0.07 | 1.8 | −0.24 | 0.60 |
| | 26.55 | 202 | 2.41 | 33.27 | 0.27 | 2.30 | – | 0.00 | 0.07 | 3.2 | −0.83 | 0.63 |
| | 26.90 | 403 | 3.20 | 33.78 | −0.29 | 2.84 | – | 0.04 | 0.08 | 2.9 | 0.30 | 0.71 |
| | 27.10 | 605 | 3.45 | 34.07 | −0.55 | 3.13 | – | 0.09 | 0.08 | 2.4 | 1.05 | 0.75 |
| | 27.41 | 1010 | 2.74 | 34.37 | −0.55 | 3.27 | – | 0.25 | 0.08 | 1.0 | 1.69 | 0.77 |
| 41.5°N April | 26.11 | 0 | 2.96 | 32.77 | 1.48 | 0.99 | – | −0.24 | 0.05 | 5.3 | −2.34 | 0.49 |
| | 26.32 | 50 | 2.32 | 32.97 | 0.89 | 1.81 | – | 0.08 | 0.06 | 2.6 | −0.24 | 0.57 |
| | 26.42 | 75 | 1.61 | 33.03 | 0.80 | 1.86 | – | 0.04 | 0.06 | 2.9 | −1.26 | 0.58 |
| | 26.45 | 100 | 1.44 | 33.06 | 0.70 | 1.90 | – | −0.01 | 0.06 | 3.3 | −1.84 | 0.58 |
| | 26.57 | 150 | 2.05 | 33.26 | 0.42 | 2.13 | – | −0.04 | 0.07 | 3.6 | −1.51 | 0.61 |
| | 26.76 | 200 | 3.04 | 33.59 | −0.39 | 2.74 | – | −0.17 | 0.08 | 4.7 | −1.65 | 0.69 |
| | 26.95 | 300 | 3.34 | 33.86 | −0.71 | 3.08 | – | −0.12 | 0.08 | 4.3 | −0.96 | 0.74 |
| | 27.06 | 400 | 3.31 | 33.99 | −0.67 | 3.12 | – | −0.04 | 0.08 | 3.6 | −0.29 | 0.75 |
| | 27.14 | 500 | 3.26 | 34.09 | −0.70 | 3.11 | – | −0.08 | 0.08 | 4.0 | −0.71 | 0.75 |
| | 27.22 | 600 | 3.18 | 34.18 | −0.58 | 3.09 | – | 0.02 | 0.08 | 3.0 | 0.15 | 0.74 |
| | 27.33 | 800 | 2.88 | 34.29 | −0.65 | 3.09 | – | −0.05 | 0.08 | 3.6 | −0.76 | 0.74 |
| 38.5°N April | 25.41 | 0 | 16.06 | 34.58 | 0.90 | 0.22 | – | −1.66 | 0.05 | 17.7 | −1.62 | 0.46 |
| | 25.41 | 10 | 16.06 | 34.58 | 0.95 | 0.25 | – | −1.58 | 0.05 | 17.0 | −0.93 | 0.46 |
| | 25.41 | 30 | 16.06 | 34.57 | 1.00 | 0.24 | – | −1.54 | 0.05 | 16.6 | −0.58 | 0.46 |
| | 25.68 | 50 | 14.79 | 34.56 | 0.62 | 0.73 | – | −1.38 | 0.05 | 15.2 | −0.43 | 0.48 |
| | 26.04 | 75 | 12.57 | 34.44 | 0.57 | 0.99 | – | −1.14 | 0.05 | 13.1 | −0.58 | 0.49 |
| | 26.16 | 100 | 11.72 | 34.37 | 0.54 | 1.04 | – | −1.12 | 0.05 | 13.0 | −1.29 | 0.50 |
| | 26.27 | 200 | 10.53 | 34.24 | 0.64 | 0.81 | – | −1.26 | 0.05 | 14.2 | −3.70 | 0.48 |
| | 26.50 | 300 | 5.42 | 33.57 | 0.65 | 1.11 | – | −0.93 | 0.05 | 11.3 | −5.88 | 0.50 |
| | 26.62 | 400 | 4.96 | 33.66 | 0.35 | 1.66 | – | −0.62 | 0.06 | 8.6 | −3.68 | 0.55 |
| | 26.78 | 500 | 3.23 | 33.63 | −0.11 | 2.44 | – | −0.23 | 0.07 | 5.2 | −1.99 | 0.65 |
| | 26.96 | 600 | 4.50 | 34.02 | −0.32 | 2.65 | – | −0.21 | 0.07 | 5.1 | −0.57 | 0.68 |
| | 27.19 | 800 | 3.68 | 34.21 | −0.46 | 2.98 | – | 0.02 | 0.08 | 3.1 | 0.62 | 0.73 |
| | 27.33 | 1000 | 3.27 | 34.32 | −0.50 | 3.04 | – | 0.05 | 0.08 | 2.8 | 0.47 | 0.74 |
| 35°N April | 24.79 | 0 | 19.12 | 34.74 | 1.07 | 0.05 | – | −1.67 | 0.05 | 17.8 | 1.31 | 0.46 |
| | 24.81 | 50 | 19.09 | 34.75 | | 0.08 | – | | | | | |
| | 25.08 | 100 | 18.09 | 34.78 | | 0.11 | – | | | | | |
| | 25.25 | 200 | 17.30 | 34.74 | 0.80 | 0.35 | – | −1.61 | 0.05 | 17.3 | 0.02 | 0.46 |
| | 25.58 | 300 | 15.60 | 34.65 | 0.64 | 0.65 | – | −1.45 | 0.05 | 15.8 | −0.25 | 0.47 |
| | 25.99 | 400 | 13.03 | 34.48 | 0.54 | 0.96 | – | −1.20 | 0.05 | 13.7 | −0.64 | 0.49 |
| | 26.38 | 500 | 10.38 | 34.33 | 0.32 | 1.52 | – | −0.82 | 0.06 | 10.3 | 0.04 | 0.54 |

**Table A1.** (continued)

| Station | Pot. Density $\sigma_\theta$ | Depth, m | $T_{pot}$, °C | Salinity, psu | $\delta^{13}C$, ‰ PDB | $PO_4^{3-}$, μmol/kg | Error ±1σ | $\delta^{13}C_{as}$, ‰ | Error ±1σ | $T_{iso}$, °C | ΔT, °C | Error ±1σ |
|---|---|---|---|---|---|---|---|---|---|---|---|---|
| | 26.68 | 600 | 8.15 | 34.26 | 0.19 | 1.64 | – | −0.81 | 0.06 | 10.3 | −2.10 | 0.55 |
| | 26.84 | 700 | 6.46 | 34.16 | 0.06 | 2.11 | – | −0.42 | 0.07 | 6.9 | −0.45 | 0.61 |
| | 26.99 | 800 | 5.06 | 34.14 | −0.13 | 2.26 | – | −0.45 | 0.07 | 7.1 | −2.07 | 0.63 |
| | 27.11 | 900 | 5.05 | 34.29 | −0.10 | 2.61 | – | −0.04 | 0.07 | 3.5 | 1.51 | 0.67 |
| | 27.22 | 1000 | 4.34 | 34.33 | −0.18 | 2.60 | – | −0.12 | 0.07 | 4.2 | 0.10 | 0.67 |
| | 27.39 | 1200 | 3.14 | 34.38 | −0.36 | 3.09 | – | 0.23 | 0.08 | 1.2 | 1.95 | 0.74 |
| 36°N April | 24.60 | 0 | 19.87 | 34.74 | | 0.05 | – | | | | | |
| | 24.67 | 50 | 19.67 | 34.76 | | 0.10 | – | | | | | |
| | 24.89 | 100 | 18.97 | 34.81 | 0.93 | 0.19 | – | −1.66 | 0.05 | 17.7 | 1.29 | 0.46 |
| | 25.34 | 200 | 16.72 | 34.67 | 0.74 | 0.50 | – | −1.51 | 0.05 | 16.4 | 0.31 | 0.47 |
| | 25.83 | 300 | 14.11 | 34.55 | | 0.95 | – | | | | | |
| | 26.29 | 400 | 10.89 | 34.34 | 0.35 | 1.33 | – | −0.99 | 0.06 | 11.8 | −0.96 | 0.52 |
| | 26.63 | 500 | 8.21 | 34.22 | 0.06 | 1.86 | – | −0.70 | 0.06 | 9.3 | −1.07 | 0.58 |
| | 26.89 | 600 | 5.89 | 34.13 | −0.04 | 2.39 | – | −0.21 | 0.07 | 5.1 | 0.80 | 0.64 |
| | 27.08 | 700 | 4.97 | 34.23 | −0.21 | 2.49 | – | −0.28 | 0.07 | 5.7 | −0.71 | 0.66 |
| | 27.19 | 800 | 4.31 | 34.28 | −0.24 | 2.75 | – | −0.02 | 0.08 | 3.4 | 0.91 | 0.69 |
| | 27.29 | 900 | 3.70 | 34.33 | −0.26 | 2.87 | – | 0.11 | 0.08 | 2.3 | 1.39 | 0.71 |
| | 27.37 | 1000 | 3.45 | 34.40 | −0.31 | 2.80 | – | −0.03 | 0.08 | 3.5 | −0.01 | 0.70 |
| | 27.44 | 1200 | 3.04 | 34.44 | −0.27 | 2.85 | – | 0.07 | 0.08 | 2.6 | 0.39 | 0.71 |
| 42°N August | 24.60 | 0 | 12.16 | 32.47 | 2.26 | 0.49 | 0.48 | −0.01 | 0.05 | 3.3 | 8.81 | 0.47 |
| | 25.07 | 10 | 9.26 | 32.44 | | 0.65 | 0.64 | | | | | |
| | 26.10 | 30 | 3.84 | 32.86 | 1.34 | 1.57 | 1.53 | 0.22 | 0.06 | 1.3 | 2.53 | 0.55 |
| | 26.34 | 50 | 2.44 | 33.01 | 1.15 | 1.76 | – | 0.28 | 0.06 | 0.8 | 1.63 | 0.57 |
| | 26.45 | 75 | 1.14 | 33.03 | 0.59 | 1.87 | 1.82 | −0.20 | 0.06 | 5.0 | −3.84 | 0.58 |
| | 26.47 | 100 | 1.44 | 33.08 | 0.41 | 1.91 | – | −0.28 | 0.06 | 5.7 | −4.22 | 0.58 |
| | 26.58 | 125 | 1.29 | 33.20 | 0.36 | 2.08 | 2.03 | −0.21 | 0.07 | 5.1 | −3.79 | 0.60 |
| | 26.60 | 150 | 1.79 | 33.27 | 0.24 | 2.12 | – | −0.23 | 0.07 | 5.2 | −3.44 | 0.61 |
| | 26.64 | 175 | 1.72 | 33.31 | | 2.25 | 2.19 | | | | | |
| | 26.70 | 250 | 1.86 | 33.40 | 0.01 | 2.35 | 2.29 | −0.22 | 0.07 | 5.1 | −3.25 | 0.63 |
| | 26.76 | 300 | 1.74 | 33.47 | −0.09 | 2.40 | 2.34 | −0.21 | 0.07 | 5.1 | −3.33 | 0.64 |
| | 26.85 | 400 | 1.74 | 33.58 | −0.13 | 2.50 | 2.44 | −0.17 | 0.07 | 4.7 | −2.93 | 0.65 |
| | 26.96 | 500 | 2.46 | 33.78 | −0.45 | 2.58 | 2.51 | −0.22 | 0.07 | 5.2 | −2.70 | 0.67 |
| | 27.09 | 600 | 3.22 | 34.02 | −0.46 | 2.98 | – | 0.02 | 0.08 | 3.1 | 0.14 | 0.73 |
| | 27.18 | 700 | 3.26 | 34.14 | −0.52 | 3.06 | 2.98 | −0.01 | 0.08 | 3.3 | −0.02 | 0.73 |
| | 27.26 | 800 | 3.06 | 34.22 | −0.60 | 3.10 | 3.01 | 0.09 | 0.08 | 2.5 | 0.57 | 0.74 |
| | 27.39 | 1000 | 2.78 | 34.35 | | 3.26 | 3.17 | | | | | |
| 40°N August | 23.36 | 0 | 20.25 | 33.24 | | 0.11 | 0.11 | | | | | |
| | 23.51 | 12 | 19.19 | 33.08 | 2.09 | 0.16 | 0.15 | −0.54 | 0.05 | 8.0 | 11.24 | 0.46 |
| | 25.58 | 31 | 12.02 | 33.71 | 1.35 | 0.71 | 0.69 | −0.69 | 0.05 | 9.2 | 2.77 | 0.48 |
| | 26.15 | 49 | 9.37 | 33.84 | 0.67 | 1.33 | 1.30 | −0.70 | 0.06 | 9.3 | 0.04 | 0.52 |
| | 26.46 | 75 | 4.57 | 33.41 | 0.72 | 1.67 | 1.63 | −0.29 | 0.06 | 5.7 | −1.15 | 0.55 |
| | 26.53 | 100 | 4.15 | 33.44 | 0.57 | 1.97 | 1.92 | −0.12 | 0.06 | 4.3 | −0.15 | 0.59 |
| | 26.56 | 123 | 3.80 | 33.43 | 0.50 | 1.69 | 1.65 | −0.49 | 0.06 | 7.5 | −3.68 | 0.56 |
| | 26.57 | 151 | 3.06 | 33.36 | 0.45 | 1.80 | 1.75 | −0.42 | 0.06 | 6.9 | −3.84 | 0.57 |
| | 26.62 | 175 | 2.59 | 33.37 | 0.43 | 2.04 | 1.99 | −0.18 | 0.06 | 4.8 | −2.25 | 0.60 |
| | 26.62 | 200 | 2.30 | 33.34 | 0.31 | 1.97 | 1.92 | −0.38 | 0.06 | 6.5 | −4.20 | 0.59 |
| | 26.69 | 250 | 2.45 | 33.44 | 0.11 | 2.33 | 2.27 | −0.20 | 0.07 | 5.0 | −2.51 | 0.63 |
| | 26.75 | 299 | 2.44 | 33.52 | −0.10 | 2.45 | 2.39 | −0.28 | 0.07 | 5.6 | −3.19 | 0.65 |
| | 26.88 | 400 | 2.93 | 33.73 | −0.27 | 2.73 | 2.66 | −0.14 | 0.07 | 4.4 | −1.50 | 0.69 |
| | 27.01 | 498 | 3.26 | 33.93 | −0.57 | 2.96 | 2.88 | −0.20 | 0.08 | 5.0 | −1.72 | 0.72 |
| | 27.13 | 600 | 3.35 | 34.09 | −0.63 | 3.05 | 2.97 | −0.16 | 0.08 | 4.6 | −1.25 | 0.73 |
| | 27.24 | 701 | 3.10 | 34.20 | −0.63 | 3.11 | 3.03 | −0.10 | 0.08 | 4.1 | −0.97 | 0.74 |
| | 27.27 | 798 | 3.02 | 34.23 | −0.60 | 3.12 | 3.03 | −0.07 | 0.08 | 3.8 | −0.80 | 0.74 |
| | 27.38 | 1000 | 2.88 | 34.35 | −0.53 | 3.06 | 2.97 | −0.06 | 0.08 | 3.8 | −0.87 | 0.73 |
| | 27.49 | 1249 | 2.50 | 34.44 | −0.48 | 3.04 | 2.96 | −0.02 | 0.08 | 3.4 | −0.90 | 0.73 |
| | 27.56 | 1499 | 2.27 | 34.51 | −0.51 | 3.02 | 2.94 | −0.08 | 0.08 | 3.9 | −1.64 | 0.73 |
| 38.5°N August | 22.81 | 0 | 23.97 | 33.90 | | 0.05 | 0.05 | | | | | |
| | 22.81 | 9 | 23.98 | 33.90 | 1.60 | 0.07 | 0.06 | −1.13 | 0.05 | 13.0 | 10.95 | 0.46 |
| | 24.90 | 49 | 16.17 | 33.94 | 1.36 | 0.17 | 0.16 | −1.26 | 0.05 | 14.2 | 1.97 | 0.46 |
| | 25.69 | 97 | 13.94 | 34.33 | 0.69 | 0.77 | 0.75 | −1.29 | 0.05 | 14.4 | −0.50 | 0.48 |
| | 25.93 | 123 | 12.61 | 34.29 | 0.63 | 0.87 | 0.85 | −1.24 | 0.05 | 14.0 | −1.40 | 0.49 |
| | 26.08 | 151 | 11.45 | 34.21 | 0.55 | 0.95 | 0.93 | −1.23 | 0.05 | 14.0 | −2.51 | 0.49 |
| | 26.22 | 174 | 10.99 | 34.27 | 0.47 | 1.21 | 1.17 | −1.03 | 0.06 | 12.2 | −1.24 | 0.51 |
| | 26.33 | 199 | 10.21 | 34.24 | 0.43 | 1.34 | 1.30 | −0.94 | 0.06 | 11.4 | −1.23 | 0.52 |
| | 26.53 | 249 | 8.55 | 34.15 | 0.38 | 1.63 | 1.59 | −0.67 | 0.06 | 9.1 | −0.52 | 0.55 |
| | 26.62 | 299 | 5.50 | 33.73 | 0.44 | 1.61 | 1.57 | −0.63 | 0.06 | 8.7 | −3.20 | 0.55 |
| | 26.74 | 398 | 4.63 | 33.76 | 0.18 | 2.22 | 2.17 | −0.24 | 0.07 | 5.3 | −0.72 | 0.62 |
| | 26.92 | 499 | 5.31 | 34.09 | −0.07 | 2.44 | 2.38 | −0.26 | 0.07 | 5.5 | −0.18 | 0.65 |
| | 27.04 | 598 | 4.39 | 34.11 | −0.20 | 2.74 | 2.66 | −0.07 | 0.07 | 3.8 | 0.58 | 0.69 |
| | 27.15 | 700 | 3.74 | 34.16 | −0.42 | 2.93 | 2.85 | −0.08 | 0.08 | 4.0 | −0.22 | 0.71 |
| | 27.25 | 799 | 3.55 | 34.26 | −0.42 | 2.93 | 2.85 | −0.09 | 0.08 | 4.0 | −0.42 | 0.71 |
| | 27.37 | 1000 | 3.06 | 34.36 | −0.43 | 3.01 | 2.93 | 0.00 | 0.08 | 3.3 | −0.21 | 0.73 |

**Table A1.** (continued)

| Station | Pot. Density $\sigma_0$ | Depth, m | $T_{pot.}$, °C | Salinity, psu | $\delta^{13}C$, ‰ PDB | $PO_4^{3-}$, μmol/kg | Error ±1σ | $\delta^{13}C_{as}$, ‰ | Error ±1σ | $T_{iso}$, °C | ΔT, °C | Error ±1σ |
|---|---|---|---|---|---|---|---|---|---|---|---|---|
| | 27.48 | 1249 | 2.69 | 34.45 | −0.38 | 3.02 | 2.94 | 0.05 | 0.08 | 2.8 | −0.13 | 0.73 |
| | 27.56 | 1499 | 2.38 | 34.51 | −0.40 | 3.00 | 2.91 | 0.00 | 0.08 | 3.2 | −0.84 | 0.72 |
| 35°N August | 21.85 | 0 | 28.14 | 34.33 | | 0.04 | 0.03 | | | | | |
| | 21.84 | 10 | 28.16 | 34.33 | 1.32 | 0.04 | 0.04 | −1.44 | 0.05 | 15.7 | 12.43 | 0.46 |
| | 22.12 | 30 | 27.31 | 34.34 | | 0.03 | 0.03 | | | | | |
| | 22.93 | 50 | 24.83 | 34.39 | | 0.05 | 0.05 | | | | | |
| | 23.60 | 75 | 22.98 | 34.54 | | 0.07 | 0.07 | | | | | |
| | 24.29 | 100 | 21.12 | 34.76 | 0.96 | 0.24 | 0.24 | −1.57 | 0.05 | 16.9 | 4.18 | 0.46 |
| | 24.63 | 124 | 19.85 | 34.77 | | 0.30 | 0.29 | | | | | |
| | 24.85 | 152 | 19.12 | 34.80 | | 0.37 | 0.36 | | | | | |
| | 25.06 | 175 | 18.34 | 34.82 | | 0.42 | 0.41 | | | | | |
| | 25.20 | 198 | 17.64 | 34.78 | 0.73 | 0.41 | 0.40 | −1.64 | 0.05 | 17.5 | 0.17 | 0.47 |
| | 25.51 | 248 | 15.94 | 34.67 | | 0.67 | 0.65 | | | | | |
| | 25.74 | 301 | 14.68 | 34.60 | 0.65 | 0.80 | 0.78 | −1.29 | 0.05 | 14.4 | 0.23 | 0.48 |
| | 26.19 | 399 | 11.68 | 34.40 | 0.42 | 1.22 | 1.19 | −1.06 | 0.06 | 12.5 | −0.82 | 0.51 |
| | 26.56 | 500 | 8.20 | 34.12 | 0.30 | 1.57 | 1.53 | −0.82 | 0.06 | 10.4 | −2.17 | 0.54 |
| | 26.78 | 602 | 6.44 | 34.09 | 0.08 | 2.07 | 2.01 | −0.50 | 0.07 | 7.6 | −1.18 | 0.60 |
| | 26.95 | 701 | 5.53 | 34.15 | −0.09 | 2.38 | 2.32 | −0.34 | 0.07 | 6.2 | −0.66 | 0.64 |
| | 27.10 | 805 | 4.64 | 34.21 | −0.24 | 2.66 | 2.59 | −0.19 | 0.07 | 4.9 | −0.28 | 0.68 |
| | 27.28 | 1001 | 3.73 | 34.32 | −0.34 | 2.93 | 2.85 | 0.00 | 0.08 | 3.3 | 0.46 | 0.71 |
| | 27.41 | 1249 | 2.90 | 34.38 | | 2.98 | 2.90 | | | | | |
| | 27.51 | 1492 | 2.53 | 34.46 | −0.39 | 3.03 | 2.95 | 0.05 | 0.08 | 2.8 | −0.27 | 0.73 |
| J33 September | 24.31 | 0 | 18.83 | 34.01 | 1.24 | 0.06 | – | −1.50 | 0.05 | 16.3 | 2.56 | 0.46 |
| | 24.31 | 10 | 18.84 | 34.02 | 1.22 | 0.04 | – | −1.53 | 0.05 | 16.6 | 3.57 | 0.46 |
| | 24.50 | 23 | 17.73 | 33.91 | 1.22 | 0.12 | – | −1.61 | 0.05 | 17.2 | 0.49 | 0.46 |
| | 25.54 | 31 | 14.48 | 34.29 | 1.05 | 0.16 | – | −1.57 | 0.05 | 16.9 | −1.11 | 0.46 |
| | 25.97 | 37 | 12.33 | 34.29 | 0.77 | 0.22 | – | −1.79 | 0.05 | 18.8 | −6.47 | 0.46 |
| | 26.17 | 54 | 11.16 | 34.26 | 0.47 | 0.30 | – | −1.99 | 0.05 | 20.6 | −9.44 | 0.46 |
| | 26.42 | 64 | 9.41 | 34.19 | 0.42 | 0.45 | – | −1.88 | 0.05 | 19.6 | −10.22 | 0.47 |
| | 26.66 | 100 | 7.77 | 34.17 | 0.40 | 0.62 | – | −1.72 | 0.05 | 18.2 | −10.40 | 0.47 |
| | 26.98 | 150 | 4.70 | 34.08 | −0.03 | 0.79 | – | −1.96 | 0.05 | 20.3 | −15.58 | 0.48 |
| | 27.17 | 200 | 2.53 | 34.06 | 0.05 | 1.08 | – | −1.57 | 0.05 | 16.9 | −14.33 | 0.50 |
| J33 April | 26.74 | 0 | 6.06 | 33.98 | 0.80 | 0.33 | – | −1.63 | 0.05 | 17.4 | −11.37 | 0.46 |
| | 26.74 | 5 | 6.06 | 33.98 | 0.75 | 0.35 | – | −1.66 | 0.05 | 17.7 | −11.64 | 0.46 |
| | 26.75 | 15 | 6.02 | 33.98 | 0.69 | 0.35 | – | −1.73 | 0.05 | 18.3 | −12.26 | 0.46 |
| | 26.77 | 24 | 5.95 | 34.00 | 0.78 | 0.35 | – | −1.64 | 0.05 | 17.5 | −11.53 | 0.46 |
| | 26.80 | 31 | 5.76 | 34.01 | 0.78 | 0.37 | – | −1.62 | 0.05 | 17.3 | −11.55 | 0.46 |
| | 26.87 | 55 | 5.37 | 34.04 | 0.61 | 0.48 | – | −1.66 | 0.05 | 17.7 | −12.34 | 0.47 |
| | 26.89 | 65 | 5.23 | 34.05 | 0.59 | 0.48 | – | −1.68 | 0.05 | 17.9 | −12.67 | 0.47 |
| | 26.96 | 100 | 4.73 | 34.06 | 0.52 | 0.55 | – | −1.68 | 0.05 | 17.8 | −13.11 | 0.47 |
| | 27.06 | 150 | 3.83 | 34.07 | 0.29 | 0.79 | – | −1.65 | 0.05 | 17.6 | −13.74 | 0.48 |
| | 27.17 | 200 | 2.42 | 34.05 | 0.16 | 1.23 | – | −1.29 | 0.06 | 14.5 | −12.04 | 0.51 |
| HS13 | 24.66 | 9 | 11.51 | 32.51 | 2.38 | 0.41 | – | 0.03 | 0.05 | 3.0 | 8.55 | 0.47 |
| | 26.43 | 50 | 0.58 | 32.98 | 1.03 | 1.53 | – | −0.09 | 0.06 | 4.0 | −3.41 | 0.54 |
| | 26.58 | 100 | 0.37 | 33.17 | 0.72 | 1.88 | – | −0.01 | 0.06 | 3.3 | −2.96 | 0.58 |
| | 26.65 | 150 | 0.24 | 33.26 | 0.35 | 2.07 | – | −0.17 | 0.07 | 4.7 | −4.50 | 0.60 |
| | 26.70 | 200 | 1.04 | 33.40 | 0.24 | 2.34 | – | 0.01 | 0.07 | 3.1 | −2.07 | 0.64 |
| | 26.78 | 301 | 1.40 | 33.51 | −0.03 | 2.54 | – | −0.04 | 0.07 | 3.5 | −2.15 | 0.66 |
| | 26.83 | 400 | 1.51 | 33.60 | −0.11 | 2.66 | – | 0.02 | 0.07 | 3.1 | −1.58 | 0.68 |
| | 26.97 | 599 | 2.09 | 33.90 | −0.32 | 2.74 | – | −0.11 | 0.08 | 4.2 | −2.06 | 0.69 |
| | 27.20 | 800 | 2.40 | 34.18 | −0.43 | 2.89 | – | −0.05 | 0.08 | 3.7 | −1.27 | 0.71 |
| | 27.35 | 1001 | 2.38 | 34.33 | −0.42 | 2.95 | – | 0.03 | 0.08 | 3.0 | −0.64 | 0.72 |
| HS9 | 24.60 | 9.5 | 12.11 | 32.46 | | 0.47 | – | | | | | |
| | 26.30 | 50 | 2.28 | 32.94 | 0.97 | 1.24 | – | −0.47 | 0.06 | 7.3 | −5.01 | 0.51 |
| | 26.58 | 100 | 1.00 | 33.17 | 0.63 | 1.58 | – | −0.43 | 0.06 | 7.0 | −5.99 | 0.55 |
| | 26.67 | 150 | 1.11 | 33.30 | 0.56 | 2.03 | – | −0.01 | 0.06 | 3.3 | −2.18 | 0.60 |
| | 26.73 | 200 | 1.50 | 33.40 | 0.36 | 2.12 | – | −0.11 | 0.07 | 4.2 | −2.68 | 0.61 |
| | 26.79 | 300 | 1.12 | 33.45 | 0.24 | 2.22 | – | −0.12 | 0.07 | 4.3 | −3.14 | 0.62 |
| | 26.85 | 400 | 1.16 | 33.53 | 0.28 | 2.35 | – | 0.07 | 0.07 | 2.7 | −1.50 | 0.64 |
| | 27.06 | 600 | 1.88 | 33.85 | −0.15 | 2.56 | – | −0.13 | 0.07 | 4.4 | −2.52 | 0.67 |
| | 27.25 | 800 | 2.19 | 34.11 | −0.15 | 2.93 | – | 0.27 | 0.08 | 0.9 | 1.34 | 0.72 |
| | 27.38 | 1000 | 2.32 | 34.28 | −0.39 | 2.99 | – | 0.10 | 0.08 | 2.4 | −0.04 | 0.73 |
| | 27.46 | 1060 | 2.32 | 34.38 | −0.33 | 2.94 | – | 0.10 | 0.08 | 2.3 | 0.00 | 0.72 |

[36] In conclusion, this study indicates that the $\delta^{13}C_{as}$ is useful in exploring the flow paths of intermediate waters around the western North Pacific and its marginal seas and may be applicable to other similar intermediate waters.

## Appendix A

[37] The data in Table A1 are generated from the present study. Data on stations HS9 and HS13 are cited from http://whpo.ucsd.edu/data/onetime/pacific/p01/p01w/index.htm and *Keigwin* [1998]. Standard deviation for phosphate concentration is calculated with the relationship obtained with duplicate analysis during the cruise of R/V *Soyo Maru* in August 1997. Here $\sigma_{PO4}^{3-} = 0.019 * [PO_4^{3-}] - 0.001$ ($r^2 = 0.9996$).

## References


Aota, M., Studies on the Soya warm current (in Japanese), *Teion Kagaku*, *33*, 151–172, 1975.

Bickert, T., and G. Wefer, South Atlantic and benthic foraminifer $\delta^{13}C$ deviations: Implications for reconstructing the Late Quaternary deep-water circulation, *Deep Sea Res., Part II*, *46*, 437–452, 1999.

Broecker, W. S., and E. Maier-Reimer, The influence of air and sea exchange on the carbon isotope distribution in the sea, *Global Biogeochem. Cycles*, *6*, 315–320, 1992.

Broecker, W. S., and T.-H. Peng, *Tracers in the Sea*, Lamont-Doherty Earth Obs., Palisades, N. Y., 1982.

Charles, C. D., and F. G. Fairbanks, Glacial to interglacial changes in the isotopic gradients of Southern Ocean surface waters, in *Geological History of the Polar Oceans: Arctic Versus Antarctic*, pp. 519–538, Kluwer Acad., Norwell, Mass., 1990.

Chu, P. C., J. Lan, and C. Fan, Japan Sea thermohaline structure and circulation, part I, Climatology, *J. Phys. Oceanogr.*, *31*, 244–271, 2001.

Craig, H., Isotopic standards for carbon and oxygen and correction factors for mass-spectrometric analysis of carbon dioxide, *Geochim. Cosmochim. Acta*, *12*, 133–149, 1957.

Fujii, K., and Y. Sato, Productivity and oceanographic structure in the coastal waters of the Japan Sea and Okhotsk Sea coasts of Hokkaido (in Japanese), *Bull. Jpn. Soc. Fish. Oceanogr.*, *34*, 57–62, 1979.

Itou, M., T. Ono, T. Oba, and S. Noriki, Isotopic composition and morphology of living *Globorotalia scitula*: A new proxy of sub-intermediate ocean carbonate chemistry?, *Mar. Micropaleontol.*, *421*, 189–210, 2001.

Kawai, H., Hydrography of the Kuroshio and the Oyashio, in *Physical Oceanography II*, pp. 129–320, Tokai Univ. Press, Tokyo, 1972.

Keigwin, L. D., Glacial-age hydrography of the far northwest Pacific Ocean, *Paleoceanography*, *13*, 323–339, 1998.

Levitus, S., Climatological atlas of the world ocean, *NOAA Prof. Pap. 13*, 173 pp., U. S. Govt. Print. Off., Washington, D. C., 1982.

Lynch-Stieglitz, J., and R. G. Fairbanks, A conservative tracer for glacial ocean circulation from carbon isotope and paleonutrient measurements in benthic foraminifera, *Nature*, *369*, 308–310, 1994.

Lynch-Stieglitz, J., T. F. Stocker, W. S. Broecker, and R. G. Fairbanks, The influence of air-sea exchange on the isotopic composition of oceanic carbon, observation and modeling, *Global Biogeochem. Cycles*, *9*, 653–665, 1995.

Mackensen, A., Oxygen and carbon stable isotope tracers of Weddell Sea water masses: New data and some paleoceanographic implications, *Deep Sea Res., Part I*, *48*, 1401–1422, 2001.

Mackensen, A., H.-W. Hubberten, N. Scheele, and R. Schlitzer, Decoupling of $\delta^{13}C_{\Sigma CO_2}$ and phosphate in recent Weddell Sea deep and bottom water: Implications for glacial Southern Ocean paleoceanography, *Paleoceanography*, *11*, 203–215, 1996.

Mook, W. G., J. C. Bommerson, and W. H. Staverman, Carbon isotope fractionation between dissolved bicarbonate and gaseous carbon dioxide, *Earth Planet. Sci. Lett.*, *22*, 169–176, 1974.

Ono, T., I. Yasuda, H. Narita, and S. Tsunogai, Chemical alternation of waters in the Kuroshio/Oyashio interfrontal zone, *J. Oceanogr.*, *54*, 681–694, 1998.

Rau, G. H., T. Takahashi, and D. J. DesMaris, Latitudinal variations in plankton $\delta^{13}C$: Implication for $CO_2$ and productivity in past oceans, *Nature*, *341*, 516–518, 1989.

Reid, J. L., *Intermediate Waters of the Pacific Ocean*, 85 pp., Johns Hopkins Univ. Press, Baltimore, Md., 1965.

Reid, J. L., Sea-surface temperature, salinity, and density of the Pacific Ocean in summer and in winter, *Deep Sea Res.*, *16*, Suppl., 215–224, 1969.

Stabeno, P. J., R. K. Reed, and J. E. Overland, Lagrangian measurements in the Kamchatka Current and Oyashio, *J. Oceanogr.*, *50*, 653–662, 1994.

Takizawa, T., Characteristics of the Soya Warm Current in the Okhotsk Sea, *J. Oceanogr. Soc. Jpn.*, *38*, 281–292, 1982.

Talley, L. D., Potential vorticity distribution in the North Pacific, *J. Phys. Oceanogr.*, *18*, 89–106, 1988.

Talley, L. D., An Okhotsk Sea water anomaly: Implications for ventilation in the North Pacific, *Deep Sea Res.*, *38*, 171–190, 1991.

Talley, L. D., Distribution and formation of North Pacific Intermediate Water, *J. Phys. Oceanogr.*, *23*, 517–537, 1993.

Talley, L. D., North Pacific Intermediate Water transports in the mixed water region, *J. Phys. Oceanogr.*, *27*, 1795–1803, 1997.

Tsunogai, S., S. Watanabe, M. Honda, and T. Aramaki, North Pacific intermediate water studied chiefly with radiocarbon, *J. Oceanogr.*, *51*, 519–536, 1995.

Watanabe, T., and M. Wakatsuchi, Formation of $26.8–26.9\sigma_\theta$ water in the Kuril Basin of the Sea of Okhotsk as a possible origin of North Pacific Intermediate Water, *J. Geophys. Res.*, *103*, 2849–2865, 1998.

Wong, C. S., R. J. Matear, H. J. Freeland, F. A. Whitney, and A. S. Bychkov, WOCE line P1W in the Sea of Okhotsk, 2, CFCs and the formation rate of intermediate water, *J. Geophys. Res.*, *103*, 15,625–15,642, 1998.

Yamamoto, M., S. Watanabe, S. Tsunogai, and M. Wakatsuchi, Formation of Okhotsk Sea dense shelf water and its role in the North Pacific Intermediate Water, clarified with oxygen isotopes, *Deep Sea Res., Part I*, *49*, 1165–1175, 2002.

Yasuda, I., The origin of the North Pacific Intermediate Water, *J. Geophys. Res.*, *102*, 893–909, 1997.

Zhang, J., P. D. Quay, and D. O. Wilber, Carbon isotope fractionation during gas-water exchange and dissolution of $CO_2$, *Geochim. Cosmochim. Acta*, *59*, 107–114, 1995.



M. Itou, Institute for Frontier Research on Earth Evolution, JAMSTEC, Natsushimacho 2-15, Yokosuka, Kanagawa 237-0061, Japan. (masasitou@jamstec.go.jp)

S. Noriki, Graduate School of Environmental Earth Science, Hokkaido University, Kitaku Kita 10 Nishi 5, Sapporo 060-0810, Japan.

T. Ono, Hokkaido National Fisheries Research Institute, Fisheries Research Agency, Katsuragoi 116, Kushiro, Hokkaido 085-0802, Japan.